The Appearance of Phosphenes Elicited Using a Suprachoroidal Retinal Prosthesis

Nicholas C. Sinclair,[1] Mohit N. Shivdasani,[1,2] Thushara Perera,[1,2] Lisa N. Gillespie,[1] Hugh J. McDermott,[1,2] Lauren N. Ayton,[3] and Peter J. Blamey[1,2]; for the Bionic Vision Australia Consortium

[1]Bionics Institute, East Melbourne, Australia
[2]Department of Medical Bionics, The University of Melbourne, Carlton, Australia
[3]Centre for Eye Research Australia, The University of Melbourne, Royal Victorian Eye and Ear Hospital, East Melbourne, Australia

Correspondence: Nicholas C. Sinclair, Bionics Institute, 384-388 Albert Street, East Melbourne, VIC 3002, Australia; nsinclair@bionicsinstitute.org.

See the appendix for the members of the Bionic Vision Australia Consortium.

Submitted: December 21, 2015
Accepted: August 1, 2016

Citation: Sinclair NC, Shivdasani MN, Perera T, et al.; for the Bionic Vision Australia Consortium. The appearance of phosphenes elicited using a suprachoroidal retinal prosthesis. *Invest Ophthalmol Vis Sci*. 2016;57:4948–4961. DOI:10.1167/iovs.15-18991

Purpose. Phosphenes are the fundamental building blocks for presenting meaningful visual information to the visually impaired using a bionic eye device. The aim of this study was to characterize the size, shape, and location of phosphenes elicited using a suprachoroidal retinal prosthesis.

Methods. Three patients with profound vision loss due to retinitis pigmentosa were implanted with a suprachoroidal electrode array, which was used to deliver charge-balanced biphasic constant-current pulses at various rates, amplitudes, and durations to produce phosphenes. Tasks assessing phosphene appearance, location, overlap, and the patients' ability to recognize phosphenes were performed using a custom psychophysics setup.

Results. Phosphenes were reliably elicited in all three patients, with marked differences in the reported appearances between patients and between electrodes. Phosphene shapes ranged from simple blobs to complex forms with multiple components in both space and time. Phosphene locations within the visual field generally corresponded to the retinotopic position of the stimulating electrodes. Overlap between phosphenes elicited from adjacent electrodes was observed with one patient, which reduced with increasing electrode separation. In a randomized recognition task, two patients correctly identified the electrode being stimulated for 57.2% and 23% of trials, respectively.

Conclusions. Phosphenes of varying complexity were successfully elicited in all three patients, indicating that the suprachoroidal space is an efficacious site for electrically stimulating the retina. The recognition scores obtained with two patients suggest that a suprachoroidal implant can elicit phosphenes containing unique information. This information may be useful when combining phosphenes into more complex and meaningful images that provide functional vision.

Keywords: retinal prosthesis, phosphene, suprachoroidal, bionic vision

Bionic eye devices aim to provide meaningful perception to the profoundly vision impaired through electrical stimulation of the visual system. Several sites within the visual pathway can be targeted for stimulation, including the retina,[1–5] the optic nerve,[6] the lateral geniculate nucleus,[7] and the visual cortex.[8,9] Using implanted electrode arrays, localized populations of neurons can be electrically excited to cause perception of patches of light, known as phosphenes.[10] By concurrently eliciting phosphenes with different apparent locations, it is possible to build recognizable patterns and shapes,[8,9,11–15] with the ultimate goal of creating a percept representative of the visual scene in front of the user.

As phosphenes are the fundamental building blocks for constructing detailed and meaningful bionic vision, it is important to characterize their appearance, including their size, shape, and location in the visual field, as well as how they interact. Such details may contain key information for interpreting how implantees might functionally use their phosphenes to undertake tasks and for explaining performance differences between subjects. A detailed understanding of phosphene characteristics may also identify features that can be exploited in advanced stimulation strategies and inform future device designs to improve functionality and performance.

Phosphenes elicited by electrical stimulation are typically modeled as simple, grayscale pixels whose brightness and/or size can be independently modulated to produce images in a manner similar to a dot-matrix display.[12,16,17] However, phosphenes perceived by patients have been reported to have far more complicated characteristics, including shapes varying from simple spots to lines, wedges, distorted ovals, and amorphous clouds.[2,8,9,11,15,18–20] Single-electrode stimulation has also been reported to elicit phosphenes with multiple components in space and time,[8,9,13,15,21] phosphenes that move across the visual field,[11] phosphenes with light and dark regions,[20,21] and different-colored phosphenes.[6,9,20] Furthermore, intrinsic nonlinear mapping between the visual field and the structures targeted for electrical stimulation,[22–24] as well as inadvertent activation of axonal fibers traversing the stimulation sites,[25] can distort phosphene locations in the visual field

Table 1. Patient Demographics

Patient	P1	P2	P3
Sex	Female	Male	Male
Age at implantation	52 y	49 y	63 y
Implanted eye	Left	Left	Left
Diagnosis	Retinitis pigmentosa, rod–cone dystrophy	Syndromic retinitis pigmentosa, Bardet-Beidl	Retinitis pigmentosa, rod–cone dystrophy
Years of light perception vision only, estimated	20	8–10	20
Observed degree of nystagmus	None	Moderate/severe	Severe
Level of spontaneous visual percepts/photopsia	Constant, very active	Sporadic postoperative	Sporadic
Primary mobility aid	Guide dog	Guide dog	Guide dog

and prevent them from appearing in an orderly grid that corresponds to the implanted electrode layout.[26]

The anatomic location of the stimulating electrode array is also expected to affect phosphene appearance. For example, phosphenes elicited through epiretinal stimulation have generally been described as more complex, including streak-like curved lines, wedges, and round contours,[19,25] compared to relatively well-defined round spots of light found with subretinal stimulation.[11] It is hypothesized that due to the implant locations, subretinal stimulation primarily activates the inner neural circuitry formed largely by bipolar cells, whereas epiretinal stimulation primarily activates retinal ganglion cells (RGCs) and their axons, leading to more complex percepts.

Recently, our group has pioneered a novel surgical technique whereby the electrode array is inserted into the suprachoroidal space between the choroid and the sclera and is held there in a natural cleavage plane.[5,27,28] In comparison to epiretinal and subretinal implantation sites, the suprachoroidal approach has the advantage of a simpler surgery that does not require breaching the vitreous cavity or touching the retina. Being held in the natural cleavage plane also provides long-term mechanical stability to the implant location without the need for fixation techniques such as the retinal tacks used with epiretinal devices. However, these advantages come at the expense of increased distance between the electrodes and the retinal stimulation targets, which can increase the charge levels required to elicit phosphenes and limit spatial resolution.[4,29,30] Our suprachoroidal array has been shown clinically to be stable over the first year of implantation in three profoundly vision-impaired patients with retinitis pigmentosa (RP),[5] and we have been able to reliably measure perceptual thresholds within safe charge density limits using a wide range of stimulus parameters in all three patients.[4]

The main goal of this study was to investigate the appearance and recognizability of phosphenes elicited using our prototype suprachoroidal retinal prosthesis in these three patients with profound vision loss due to RP. Tasks were performed to assess phosphene shape, size, temporal properties, location, overlap, and recognizability, as well as the influence of stimulation parameters on percept appearance. Characterization of the phosphenes produced from this implantation site provides valuable information for assessing the feasibility of using suprachoroidal electrode arrays to provide complex and meaningful visual information to patients, as well as for interpreting results from subsequent psychophysics and functional real-time, camera-driven experiments.

Materials and Methods

Patients, Implant, and Surgery

With approval from the Royal Victorian Eye and Ear Hospital Human Research Ethics Committee (application no. 11/1032H), three patients (Table 1) with end-stage RP (light perception vision only) were selected for implantation with a prototype suprachoroidal retinal prosthesis as part of the Bionic Vision Australia program. Patients were selected through a clinical screening process conducted by the Centre for Eye Research Australia that included a battery of visual function tests and clinical assessments.[5] Informed consent was obtained from all patients after explanation of the nature and possible consequences of the study. The clinical trial was registered at www.clinicaltrials.gov (trial no. NCT01603576) and adhered to the tenets of the Declaration of Helsinki.

The prototype suprachoroidal retinal prosthesis consisted of an electrode array connected via a multiwire cable to a titanium percutaneous connector (Figs. 1A, 1B). The percutaneous connector was used to provide a direct electrical connection to the implanted electrodes. This allowed maximum flexibility in the stimulation applied as it enabled the use of an external neurostimulator with greater configurability and wider-ranging specifications compared to fully implantable devices.[31] The electrode array included 20 platinum discs (17 $\times$ 600-μm and 3 $\times$ 400-μm diameter) arranged in a hexagonal grid within a silicone substrate, used primarily as active charge delivery sites. Thirteen interconnected 600-μm-diameter platinum discs positioned around the top, bottom, and inside edges of the hexagonal grid and two 2-mm-diameter platinum discs were also included for use as return electrodes. An additional platinum pin electrode was implanted near the percutaneous connector for use as a remote return. Each electrode was individually connected via a helical platinum/iridium wire to a pin of the percutaneous connector.

Details of the implantation procedure have been published previously.[4,5,27,28] In brief, the percutaneous connector and subcutaneous remote return electrode were implanted behind the ear (Fig. 1D), with the connector anchored to the temporal bone using titanium screws. The cable and electrode array were tunneled beneath the temporalis fascia to the lateral orbit margin. After a lateral canthotomy, disinserting the lateral rectus muscle and making a scleral incision, a pocket was made within the suprachoroidal space using a lens glide. The electrode array was fully inserted into the pocket, the scleral wound sutured, and the lateral rectus muscle reattached. The position of the electrode array with respect to the optic disc and the macula was assessed using indirect ophthalmoscopy and fundus imaging (Fig. 1C).

Psychophysics Setup and Stimulation

Studies to characterize phosphenes, as detailed below, were performed using a purpose-built psychophysics setup. The setup included a custom clinician interface (EyeSee) for controlling experiments, a highly configurable constant-current neurostimulator (neuroBi[31]), and devices for acquiring perceptual information from the patient, including motion-

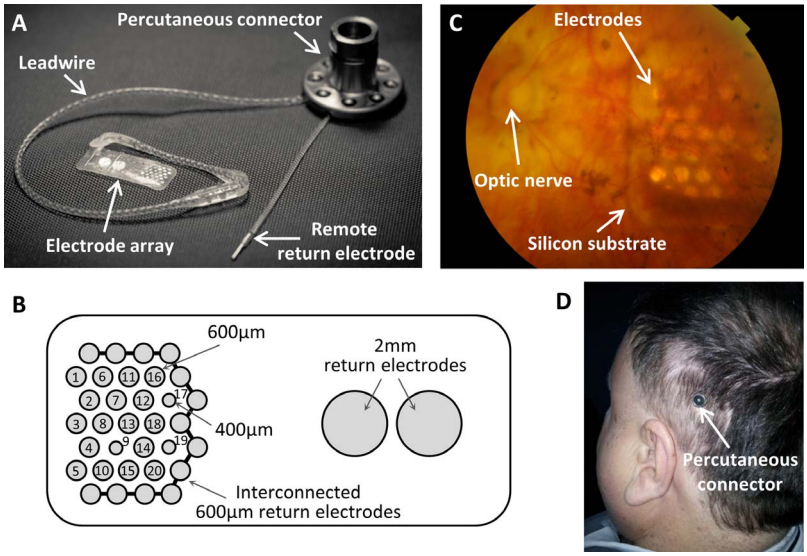

Figure 1. Prototype suprachoroidal retinal prosthesis. (**A**) The device consisted of a percutaneous connector connected via a cable to an electrode array designed to be implanted in the suprachoroidal space of the eye. (**B**) Schematic illustration of the electrode array (not to scale). Twenty stimulating electrodes (17 × 600-µm and 3 × 400-µm diameter) are arranged in a hexagonal grid, surrounded by 13 interconnected 600-µm-diameter electrodes that form a guard-ring return. Two large return electrodes (2-mm diameter) are also included in the array. (**C**) Fundus image recorded from P1. The electrode array implanted in the suprachoroidal space is visible through the retina and choroid. (**D**) The percutaneous connector is implanted behind the ear, providing a direct electrical connection to the implanted electrodes. Image in (**A**) courtesy of D.A.X. Nayagam.

tracking (Ascension Technology Corp., Shelburne, VT, USA) for tracking head and finger movements and eye-tracking (Arrington Research, Inc., Scottsdale, AZ, USA) systems. Stimulation was delivered at stepped charge levels above predetermined perceptual thresholds, measured using an iterative staircase procedure described previously.[4] The pulse phase width was fixed to a nominated value for the duration of each experiment, and the current amplitude was adjusted to deliver the required charge levels. A decibel (dB) scale was used to define stimulation levels relative to threshold, as it has been found that perceived intensity can be described as a power function of stimulation amplitude for an epiretinal visual prosthesis.[32] Stimulus magnitude was capped by a charge limit, set using the model of safe levels of electrical stimulation[33] shown by Merrill et al.[34] with a k value of 1.85.

Phosphene Appearance Task

Phosphene appearance was characterized using a combination of drawings and verbal descriptions by the patient. Stimulation was applied to a nominated electrode configuration for a fixed duration (typically 2 seconds). Immediately following the stimulus, the patient was asked to trace the outline of the perceived phosphene at arm's length using the index finger (Fig. 2A). A motion tracker sensor attached to the patient's index finger was used to capture the drawing. A second motion tracker sensor positioned above the patient's implanted eye was used as a reference point to convert the drawing from raw position coordinates to degrees of visual angle. Phosphene size for each drawing was defined as the area of visual field covered and was calculated by first plotting the data using Matlab (Mathworks, Natick, MA, USA) and then using Axiovision (Carl Zeiss AG, Oberkochen, Germany) to measure the area of the enclosed shapes in units of degrees squared (°sq) (Figs. 2B, 2C). If a phosphene had multiple spatial components, the area was calculated as the sum of the areas of the separate parts.

The patient was also asked to provide a verbal description of each phosphene, including the perceived intensity and color, as well as any temporal changes that occurred during the stimulus. The phosphene appearance task was performed multiple times with each patient, using various combinations of stimulation parameters and electrode configurations (Fig. 3;

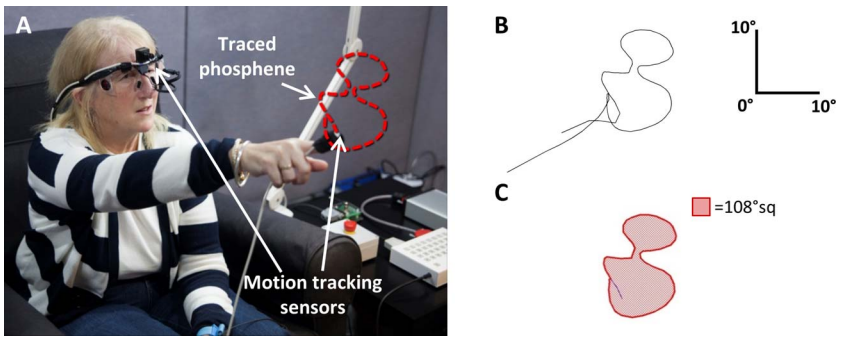

Figure 2. Phosphene drawing and area calculation. (**A**) Following stimulus presentation the patient was asked trace the outline of the perceived phosphene using the index finger. Motion tracker sensors were used to capture the drawn shape and convert it to degrees of visual angle. (**B**) The captured drawing data were then plotted. Extraneous lines caused by the patient moving the hand to/from the phosphene location were subsequently cropped. (**C**) Phosphene size was defined as the area of visual field enclosed (*shaded region*).

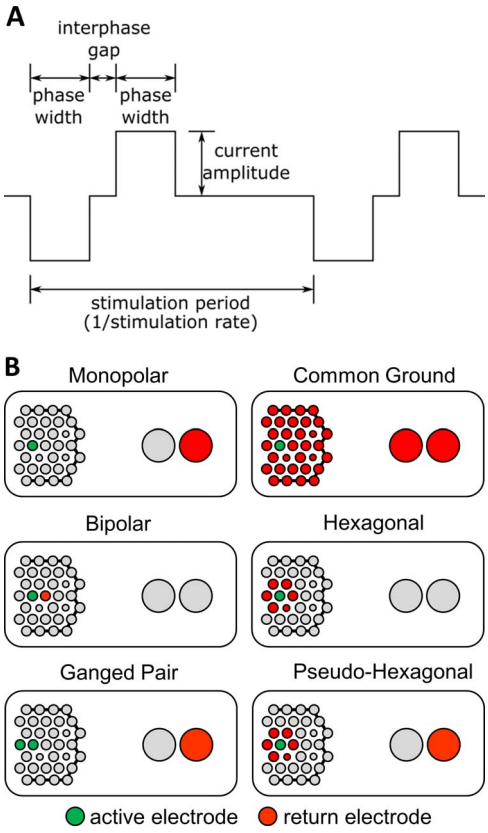

FIGURE 3. (**A**) Adjustable stimulation parameters for charge-balanced biphasic pulses. Refer to Table 2 for parameter ranges used. The pulses shown are cathodic phase first; however, anodic phase first pulses were also used. (**B**) Electrode configurations tested included monopolar (most distal 2-mm-diameter intraocular electrode used as the return), common ground (all other electrodes connected as the return), bipolar (nearby small electrode as return), hexagonal (surrounding electrodes as return[35]), ganged pair (two adjacent active electrodes connected together with the most distal 2-mm-diameter electrode used as the return), and pseudo-hexagonal (surrounding electrodes and most distal 2-mm-diameter electrode connected as the return[4,36]).

Table 2). Due to time constraints, the drawing component of the task was not performed for every combination of stimulation parameters tested; however, verbal descriptions were always obtained.

Phosphene Location Task

The perceived locations of phosphenes within the visual field were determined using a procedure similar to that used by Fujikado et al.[2] and previously used absolute mapping methods.[8,9,26] A vertical board with a tactile marker at its center was placed in front of the patient at arm's length. The patient was instructed to place his or her index finger on the tactile marker and direct his or her eyes toward the finger for the duration of the stimulus. This was done to consistently orient the patient's gaze during each trial, as eye movements have the potential to affect the perceived location of phosphenes.[37] After an individual electrode had been stimulated at a nominated level above threshold (typically between 0 and 6 dB above threshold) for a fixed duration, the patient was asked to move the index finger to the point on the board corresponding to the center of the perceived phosphene. A motion-tracking sensor attached to the patient's index finger was used to record the indicated location relative to the centrally located tactile marker. A second motion-tracking sensor positioned above the patient's implanted eye was used to convert the raw position coordinates to degrees of visual angle. The process was repeated three times for each of the 20 active electrodes in the implant (electrodes 1–20 in Fig. 1B).

TABLE 2. Stimulation Parameter Ranges Used

Parameter	Range Used
Stimulation rate	1–500 pulses per second, pps
Phase width	100 μs–1 ms
Interphase gap	20 μs–1 ms
Polarity	Anodic and cathodic phase first
Stimulus duration	0.5–20 s

Predicted phosphene locations were also estimated for comparison, based on retinotopic electrode positions. Infrared fundus imaging was used to determine the approximate center position of each electrode with respect to the fovea, using the known dimensions of the electrode array as a reference scale. Electrode positions were then translated to locations in the visual field using the formula defined by Dacey and Petersen[38] relating distance on the retina to visual angle for the Drasdo and Fowler schematic eye[23] (Fig. 4). The foveal location for each patient was determined by clinical assessment of infrared fundus images and optical coherence tomography.

Phosphene Overlap Task

The positions of phosphenes with respect to each other were further assessed using a method similar to relative mapping techniques that have been described previously.[8,26] Two individual electrodes were stimulated in a sequence to elicit two phosphenes in succession, and the patient was asked to assess whether the phosphenes were spatially separate, just touching, or distinctly overlapping. The sequence consisted of stimulating a first electrode, followed by a second electrode, and then restimulating the first electrode. The repeat of the first electrode allowed patients to confirm the consistency of their observation. Each sequence was also presented at least twice to ensure the consistency of the observed phosphene positioning. A stimulus duration of 2 seconds was used for each electrode with a 0.5-second gap in between stimuli. Patients were asked to hold their eye steady during trials to minimize the likelihood of eye movements artificially changing the perceived locations of phosphenes.

Phosphene Recognition Task

To assess the recognizability of phosphenes, individual electrodes were stimulated in a random order using a fixed set of parameters at a nominated level above threshold (typically between 0 and 6 dB above threshold). After each stimulus, the patient was asked to identify which electrode was used to elicit the phosphene. Each electrode was stimulated three times in each run of the procedure, with repeated runs performed in test sessions occurring over several weeks.

No specific phosphene recognition training was performed with the patients prior to undertaking this task. Patient ability to associate the phosphene perceived with the electrode stimulated resulted incidentally from several months' experience performing other psychophysical tasks, including threshold measurements,[4] in which they were aware of the electrode under test.

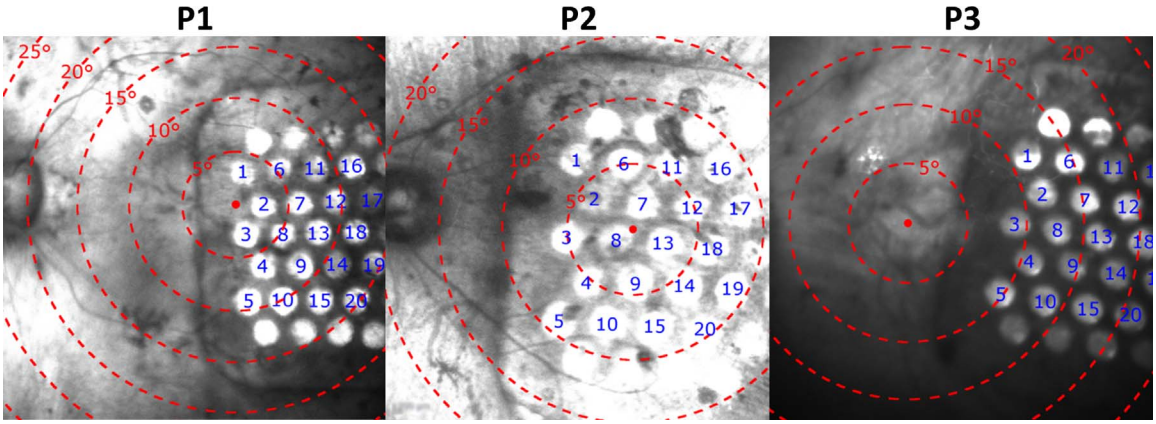

FIGURE 4. Translating electrode positions on the retina to predicted phosphene locations in the visual field using infrared fundus imaging. Predicted phosphene locations were determined by converting the distance between the fovea (*red dot at center of rings*) and each electrode center (*numbers*) into visual angle using a schematic eye model. *Dashed rings* correspond to eccentricities of visual field according to the Drasdo and Fowler schematic eye[23] in 5° increments.

RESULTS

Phosphene Appearance: Shape and Temporal Properties

The reported descriptions of phosphenes were found to be markedly different between subjects and are therefore presented on an individual basis. Phosphenes reported by patient (P)1 ranged from simple ovals filled with creamy-gray light to complex shapes with multiple light and dark components in both space and time. Figure 5 shows a representative set of phosphene drawings obtained from P1 at charge levels 2 and 6 dB above threshold (approximately 1.26× and 2× threshold) using typical stimulation settings[4] (50-pps rate, 500-μs phase width, 500-μs interphase gap, cathodic first polarity, monopolar return). Based on visual inspection, the drawings produced by P1 were very similar when stimulation was repeated using the same parameters. The simplest phosphenes were observed when stimulating electrodes that were more distant from the fovea, which was approximately located adjacent to electrode 2 (Fig. 4). Due to technical problems associated with calibrating the eye-tracking system for visually impaired subjects, use of the eye tracker was limited to monitoring the live video feed of the patient's eye. Patient 1's eye position was observed to be stable during stimulation. However, without quantitatively assessing eye position, relating patient drawings to visual space is imprecise.

Temporal changes in the intensity of phosphenes over the stimulus duration (typically 2 seconds) were generally triphasic, starting with a bright flash at the onset of stimulation followed by a duller persistent phase. For long stimulus durations (>5 seconds), the persistent component tended to fade out. No quantitative assessments, such as those used by Pérez Fornos et al.,[21] were performed to further characterize the time course of fading. Most electrodes also produced a flash at the cessation of stimulation, filled with either a multitude of light and dark spots ("sparkles") or just white light. Electrodes close to the fovea (electrodes 1–4, 6–8, 11, and 13) also exhibited dark spots during the onset flash only.

In contrast to the well-defined percepts described by P1, the phosphenes initially reported by P2 using a 50-pps stimulation rate predominantly consisted of a very brief flash at the onset of stimulation only, which was generally described as like a flare of a match that quickly disappeared. Occasionally a second flash was reported at the offset of stimulation at higher stimulation levels. However, the second flash was often reported to be in a different location in the visual field from the first flash. Upon further investigation, it was found that the different locations of the two flashes coincided with large changes in eye position that were observed over the duration of the stimulus presentation due to the subject's nystagmus. Very rarely, at higher stimulation levels (≥6 dB above threshold), P2 reported a dull flickering light ("shimmering" or "waviness") that followed the onset flash and persisted for the duration of stimulation.

Increasing the stimulation rate caused P2's phosphenes to appear brighter and increased the prevalence of the persistent dull flickering light that followed the onset flash. At high stimulation rates (>200 pps), phosphenes that persisted for the entire stimulus duration (typically 2 seconds) could be elicited from all electrodes for which a perceptual threshold could be obtained. When longer stimulus durations were used (>2 seconds), the duller persistent component tended to fade out. Onset and offset flashes were also reported to align in the visual field when higher stimulation rates were used, presumably because the persistent component further assisted the patient in maintaining focus in the area of the visual field where the phosphene was occurring. Eye gaze was also observed to be steadier when phosphenes persisted for the entire stimulus duration and enabled the patient to draw the phosphenes.

Figure 6 shows a representative set of phosphene drawings obtained from P2 using a high stimulation rate (400 pps) at a level 4 dB (approximately 1.6×) above threshold. For the stimulation parameters used (400-pps rate, 148-μs phase width, 20-μs interphase gap, anodic first polarity, monopolar return), it was not possible to elicit phosphenes within the defined safe charge limits for electrodes 17, 18, and 19 (although this was possible with other stimulation parameters). The drawings in Figure 6 correspond to the perceived onset flash, which were typically described as "blobs." The duller persistent phase was reported to replace the onset flash, occurring in the same area and appearing slightly larger.

The phosphenes reported by P3 primarily consisted of a flash at the onset of stimulation only, which was described as a short, slightly curved horizontal line that swept across the visual field. The line was consistently reported to appear to the far right, to sweep to the left and then downward toward the center of the visual field before disappearing. This same movement pattern was reported regardless of eye movements caused by the patient's nystagmus. Rarely, a flash was also

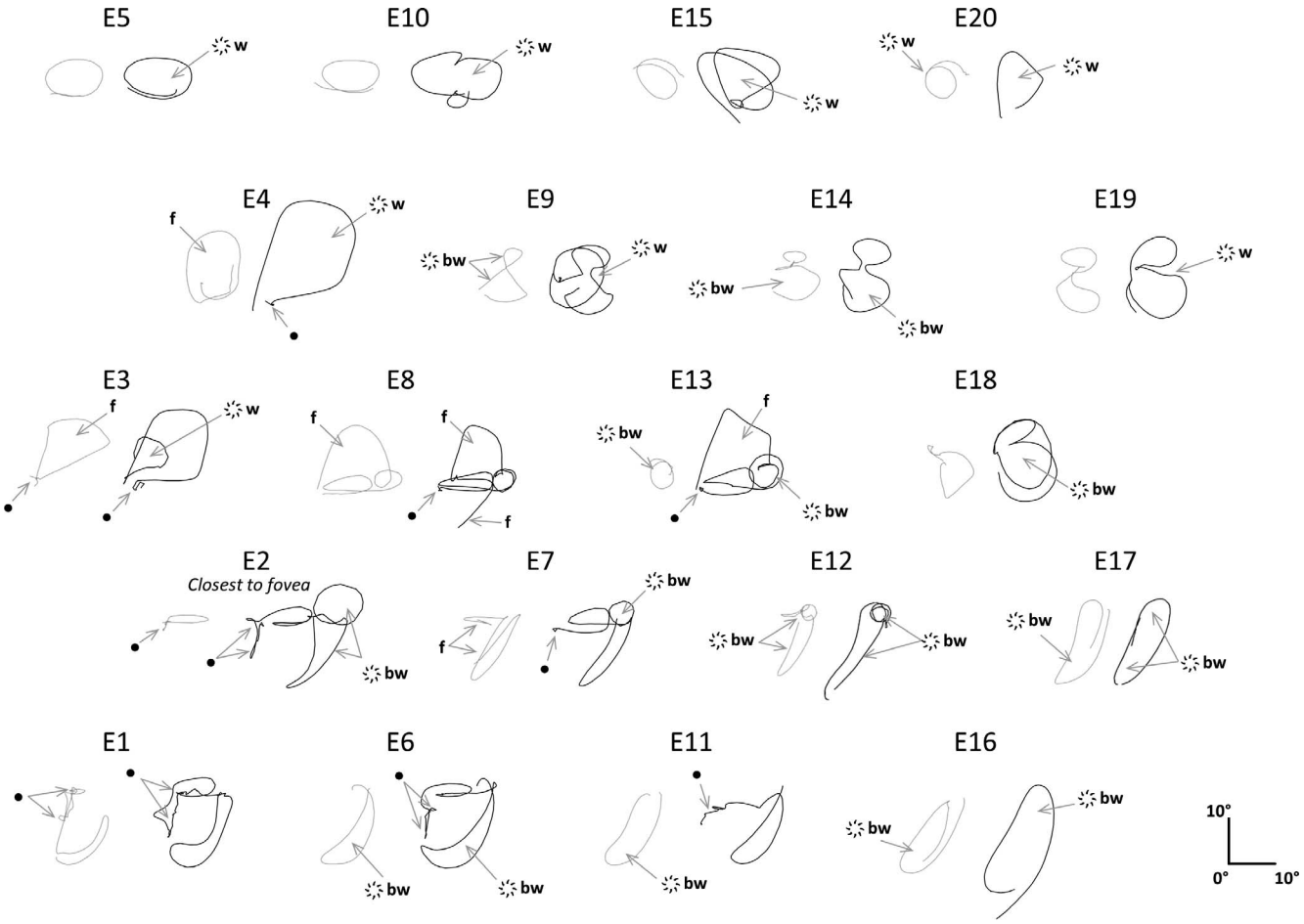

FIGURE 5. Phosphene drawings at 2 dB (*gray*) and 6 dB (*black*) above threshold for all 20 active electrodes in P1. The 2-dB drawings are displaced horizontally relative to the 6-dB drawings, and the drawings for each electrode are displaced from one another for clarity. Arrangement of drawings corresponds to electrode layout inverted to match expected position in visual field. Each drawing is to scale shown by the axes at the *lower right corner*. Enclosed shapes were reported to be filled with creamy-gray light. Phosphene areas were calculated as the sum of the areas of the enclosed shapes. Stimulation parameters: 500-μs phase width, 500-μs interphase gap, 50-pps rate, 2-second duration, cathodic phase first, monopolar configuration using a large intraocular return (rightmost 2-mm electrode in Fig. 2B). All drawings recorded 363 days postoperative. Annotations: f, very faint; •, flashed black spots at start of stimulation; w, flashed white at end of stimulation; bw, flashed black and white spots at end of stimulation. The fovea was clinically observed to be to the left of electrode 2 and the optic nerve is located to the left of the fovea (see Fig. 4).

perceived at the offset of stimulation, which was reported as the same curved line reappearing and sweeping from the center of the visual field to the right (opposite direction to the onset flash), but no visible persistent percept was reported between the onset and offset flashes. Further, these stimulation-induced phosphenes were reported to be very similar in appearance to spontaneous phosphenes that occurred sporadically. Due to the transient nature of P3's phosphenes, drawings could not be obtained.

Phosphene Appearance: Size

Increasing the stimulation charge by increasing the current amplitude caused phosphenes to appear bigger for P1 and P2. The increase in phosphene size was quantitatively assessed for P1 by calculating the areas of the visual field covered by the patient drawings. For P1, the areas of the +2-dB phosphene drawings (range, 12–178°sq; mean, 73°sq; SD, 40°sq) shown in Figure 5 were found to be significantly smaller (paired *t*-test, $P < 0.001$) than those of the +6-dB phosphene drawings (range, 59–339°sq; mean, 150°sq; SD, 64°sq). As obtaining patient drawings for each electrode was very time-consuming, a systematic and quantitative assessment of phosphene size over time for all electrodes was not possible.

Qualitatively, P1 typically reported the phosphenes to be approximately "1-2 fingers wide" (approximately 15–30 mm). Assuming that the phosphenes were perceived at arm's length, approximately 470 mm for P1, this corresponds to widths of 1.8° to 3.7°, which are far smaller than the shapes drawn. However, it should be noted that P1 found it difficult to conceptualize phosphenes as occurring at arm's length and found it challenging to relate their size at this distance.

The sizes of P1's phosphenes were reported to increase over the first year of the study period (Fig. 7). Initially, P1 anecdotally reported smaller phosphenes with shapes that were distinct from those from neighboring electrodes. Over the next 12 months, phosphenes were reported to become larger and to share features in common with phosphenes elicited from nearby electrodes. This is evident in Figure 5, where phosphenes from adjacent electrodes (e.g., electrodes 1 and 6, 2 and 7, 8 and 13) have a similar appearance. The increase in phosphene size coincided with a progressive increase in perceptual thresholds (as reported in Shivdasani et

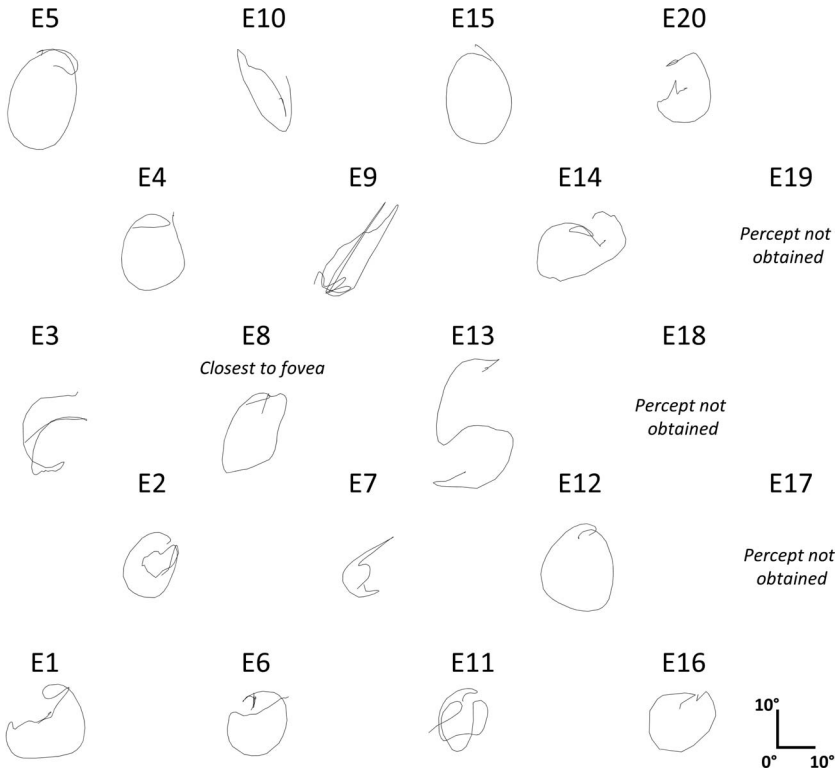

Figure 6. Phosphene drawings at 4 dB above threshold for all active electrodes in P2. Arrangement of drawings corresponds to electrode layout inverted to match expected position in visual field. Drawings are of the initial onset flash perceived, which were reported to fill the enclosed shapes with light. Following the onset flash, the patient perceived a duller shimmering light that persisted for the duration of the stimulus. The duller light was slightly larger than the onset flash and appeared in the same location. The safe charge limits set prevented percepts being obtained for electrodes 17, 18, and 19 for these stimulation parameters. Each drawing is to scale shown by the axes at the *lower right corner*. Phosphene areas were calculated as the sum of the areas of the enclosed shapes. An area was not calculated for E13 as there was not a clear enclosed shape (P2 verbally described it as an "S" shape). Stimulation parameters: 148-μs phase width, 20-μs interphase gap, 400-pps rate, 2-second duration, anodic phase first, monopolar configuration using a large intraocular return (rightmost 2-mm electrode in Fig. 2B). All drawings recorded 241 days postoperative. The fovea was clinically observed to be next to electrode 8 (see Fig. 4) and the optic nerve is located to the left of the fovea.

al.[4]) and an increase in the electrode-to-retina distance (as reported in Ayton et al.[5]). As a result, progressively higher charge levels were required over time to stimulate at the same level above threshold. The size and shape of phosphenes stabilized after the first year and did not vary notably in the final 12 months of the study.

For P2, the areas of the phosphene drawings ranged between 61°sq and 362°sq (mean, 222°sq; SD, 82°sq); however, it should be noted that P2 reported substantial difficulty in accurately drawing phosphenes to scale. Patient 2 verbally reported the sizes of phosphenes to be comparable to "10 cent" and "20 cent" Australian coins (23.6 and 28.7 mm in diameter, respectively). To further investigate the perceived size of phosphenes, in some trials immediately after a stimulus presentation P2 was asked to adjust a set of calipers to match the phosphene size. The sizes recorded ranged from 9.3 to 30 mm (average 16.2 mm) for phosphenes elicited with the same stimulation parameters as in Figure 6. Assuming that the phosphenes were perceived at arm's length, approximately 600 mm for P2, this corresponds to widths of 0.9° to 2.9° (average 1.5°), which are far smaller than the shapes traced. However, as with P1, P2 had great difficulty conceptualizing phosphenes as occurring at arm's length and could relate sizes only as he perceived them "in the eye."

As drawings could not be obtained from P3, phosphene area calculations were not possible. The transient nature of P3's phosphenes also made it difficult for him to anecdotally relate their perceived size.

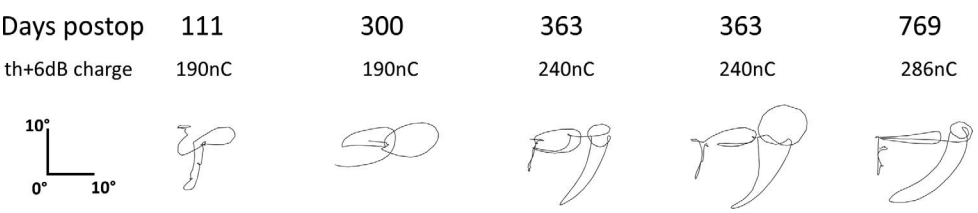

Figure 7. Changes in phosphene appearance over time for P1. All phosphene drawings shown were recorded from electrode 2 using a monopolar configuration and are scaled to the axes shown in the *lower left corner*. Phosphenes became progressively bigger over the first year of the study, coinciding with increasing perceptual thresholds, and stabilized thereafter. Two drawings are shown for 363 days postoperative to illustrate the repeatability of drawings for the same electrode, day, and stimulation level. Stimulation parameters: 500-μs phase width, 500-μs interphase gap, 50-pps rate, 2-second duration, cathodic phase first, monopolar configuration, +6 dB above threshold.

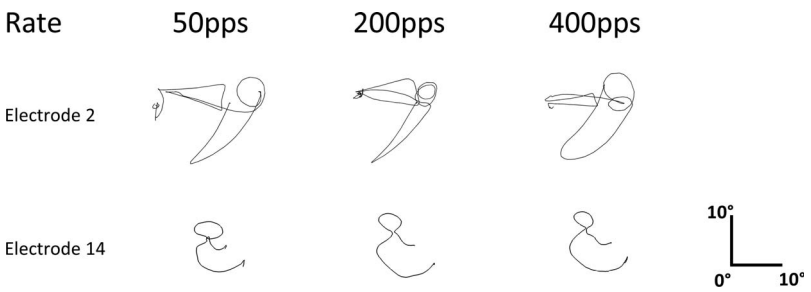

FIGURE 8. Change in phosphene appearance with stimulation rate for P1. Phosphene drawings are shown for electrodes 2 and 14. Increasing the stimulation rate did not affect the general shape; however, phosphenes were reported to appear fuller and more intense. Note: P1 reported the phosphenes for electrode 14 as closed shapes, but misaligned the start and end points of the drawings. Stimulation parameters: 148-μs phase width, 20-μs interphase gap, rate as indicated, 2-second duration, anodic phase first, monopolar configuration. Perceptual thresholds were measured for each frequency and then stimulation was applied at +6 dB above threshold. Charge levels for electrode 2 were 225 nC (50 pps), 168 nC (200 pps), and 152 nC (400 pps). Charge levels for electrode 14 were 214 nC (50 pps), 134 nC (200 pps), 128 nC (400 pps). Electrode 2 drawings were recorded 573 days postoperative, and electrode 14 drawings were recorded 594 days postoperative.

Phosphene Appearance: Effects of Stimulation Parameters

By repeating the phosphene appearance task under various stimulation conditions, the following general qualitative observations were recorded from P1:

- In addition to the increase in phosphene size reported above, increasing the stimulation level further above threshold also caused phosphenes to appear more intense.
- Increasing the stimulation rate did not strongly affect phosphene shape; however, it did cause phosphenes to appear fuller and more intense (Fig. 8).
- Shorter phase widths (≤200 μs) were reported to produce phosphenes filled with whitish-blue light, compared to the creamy-gray phosphenes produced with longer phase widths; however, the general shape, size, and temporal properties were reported to remain the same. Increasing the stimulation rate was also reported to further accentuate the change in hue, with phosphenes produced using rates ≥ 200 pps described as darker blue and purplish.
- Varying other pulse parameters (e.g., interphase gap, polarity) did not strongly affect phosphene appearance. For example, the phosphene drawings for electrode 2 shown in Figures 7 and 8 were elicited using different phase widths (148 vs. 500 μs), different interphase gaps (20 vs. 500 μs), and different polarities (anodic first versus cathodic first), yet the drawings and corresponding patient descriptions were very similar (i.e., the phosphenes obtained at 363 and 769 days postoperative in Fig. 7 have the same general shape as those for different stimulation rates in Fig. 8).
- Electrode configurations with multiple return electrodes (e.g., common ground, hexagonal, pseudo-hexagonal illustrated in Fig. 3B) did not produce markedly different phosphenes compared to a monopolar configuration, except for subtle differences in intensity (drawings not shown). Patient 1 verbally reported that phosphenes elicited using multiple return electrode configurations had the same shape as those elicited using a monopolar return, but were occasionally marginally dimmer when stimulated at the same level above threshold. This was despite these configurations having significantly higher perceptual thresholds (see Shivdasani et al.[4]).
- Bipolar electrode configurations produced percepts that were similar in appearance to the summation of the phosphenes that were elicited from the two individual electrodes using a monopolar configuration. Ganged pairs also produced percepts similar to the two individual electrode phosphenes summed together. For example, Figure 9 shows drawings of the percepts elicited using bipolar stimulation between electrodes 5 and 10, 5 and 15, and 5 and 20. When stimulated individually using a monopolar configuration, electrodes 5, 10, 15, and 20 all typically elicited a single oval or triangular shape. When stimulated as bipolar pairs, two shapes were elicited, with the separation between the two dependent on the spacing of the stimulated electrodes.

As with P1, increasing the stimulation levels further above threshold caused P2's phosphenes to appear bigger and more intense. Varying other stimulation parameters (phase width, interphase gap, polarity) and electrode configuration was reported to have little to no effect on phosphene appearance. As found with P1, it was observed that phosphenes became bigger over time, which coincided with a progressive increase in perceptual thresholds[4] and electrode-to-retina distance.[5] Higher charge levels were therefore required to stimulate at the desired levels above threshold. As the increasing charge levels approached the defined safe limits for single-electrode stimulation, in the second year of the study ganged pair electrode configurations (Fig. 3B) were predominantly used with P2 to allow higher charge levels to be delivered. The phosphenes elicited were described as having a similar blob-like appearance and onset flash followed by a duller persistent shimmering temporal progression as those produced using single-electrode monopolar stimulation.

In contrast to P1 and P2, who reported that different electrodes produced distinctly shaped phosphenes, P3 always

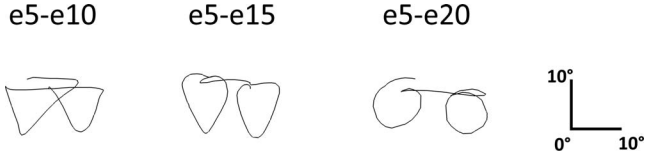

FIGURE 9. Phosphene drawings recorded from P1 using bipolar stimulation between electrodes 5 and 10, 5 and 15, and 5 and 20. When individually stimulated using a monopolar configuration, electrodes 5, 10, 15, and 20 typically produced single oval or triangular shapes. When stimulated as a bipolar pair, two shapes were elicited. The separation between shapes increased with the spacing between the stimulated electrodes. Stimulation parameters: 500-μs phase width, 500-μs interphase gap, 50-pps rate, 2-second duration, cathodic phase first. Stimulation was applied at +6 dB above threshold. Drawings were recorded 118 days postoperative.

described the same moving flash percept, and no features were identified that could be used to distinguish the phosphenes elicited using different active electrodes. When using lower stimulation rates (e.g., 50 pps), the flashes observed were described as faint and difficult to distinguish from sporadic spontaneous phosphenes. Higher stimulation rates (≥200 pps) elicited flashes that were reported to be more intense, but with the same shape and movement pattern. Increasing the stimulation level above threshold also caused the flashes to appear more intense. Varying other stimulation parameters or the return electrode configuration was not reported to affect phosphene appearance. As the charge levels required to elicit phosphenes were typically higher for P3 and approached the defined safe limits for single electrodes,[4] ganged pair electrode configurations were predominantly used with P3 to allow higher charge levels to be applied. The use of ganged pairs did not affect the reported appearance of phosphenes.

For P1 and P2, a representative set of working stimulation parameters was chosen for use in subsequent tasks. The parameters chosen were those used to create Figures 5 and 6 and are listed below. Due to the transient nature of P3's phosphenes, subsequent location, overlap, and recognition tasks could not be performed.

- Patient 1: 500-μs phase width, 500-μs interphase gap, 50-pps rate, 2-second duration, cathodic phase first, monopolar configuration
- Patient 2: 148-μs phase width, 20-μs interphase gap, 400-pps rate, 2-second duration, anodic phase first, monopolar configuration

Phosphene Location

Figure 10 illustrates the predicted and measured phosphene center locations for P1 and P2. Measured locations were obtained using the stimulation parameters corresponding to the +6-dB phosphenes shown in Figure 5 for P1 and the phosphenes shown in Figure 6 for P2. Electrodes 17, 18, and 19 were not measured for P2, as reliable phosphenes could not be elicited for those particular stimulation parameters. The measured phosphene locations for P1 occurred in an area covering 10.7° × 20.5° of the visual field, which had a greater vertical extent than the 12.7° × 11.9° area predicted from retinotopic electrode positions (Fig. 4). The measured locations for P2 occurred over an area covering 17.3° × 20.9° of the visual field, which was much larger than the predicted 12.7° × 12.5°.

While the measured locations of phosphenes were distorted from the predicted orderly grid that corresponds to the electrode array layout, for both patients, general retinotopic arrangement was observed. For example, for both patients, electrode 1 was reported to the bottom left, electrode 5 to the top left, electrode 16 to the bottom right, and electrode 20 to the top right, in accordance with the predicted locations. A somewhat vertical progression for electrodes 1 through 5 and horizontal progressions for electrodes 1, 6, 11, and 16 and electrodes 5, 10, 15, and 20 were also observed.

For both patients, the measured locations were offset to the right of the visual field compared to the predicted positions. This is particularly notable for P2, with electrode 8 measured at a horizontal visual angle of approximately 30° to the right, despite being predicted to occur at the center of the visual field due to its close proximity to the fovea.

Phosphene Overlap

The phosphene overlap task was performed with P1 for the electrode pair combinations corresponding to each horizontal row of the electrode array (e.g., 1–6, 1–11, 1–16, 6–11, 6–16, 11–16 in Fig. 1B) using the stimulation parameters that produced the +6-dB phosphenes shown in Figure 5. The pairs tested either had electrodes in adjacent columns (1 mm apart), electrodes separated by one column (2 mm apart), or electrodes separated by two columns (3 mm apart). The verbal responses from the patient were sorted into three categories: phosphenes that distinctly overlapped, phosphenes that marginally overlapped (negligible gap/overlap or phosphenes just touching), and phosphenes that were separated in space with a distinct gap in between. The results are summarized in Table 3.

The overlap task was also performed with P2; however, the results obtained from repeated runs using the same electrodes were inconsistent and are therefore not presented. It was observed that due to his nystagmus, P2 was unable to maintain a fixed gaze for the duration of the stimulation sequence (total 7 seconds). These random eye movements may have accounted for the inconsistency in the reported phosphene overlap, as eye movements are known to affect the perceived location of phosphenes.[37]

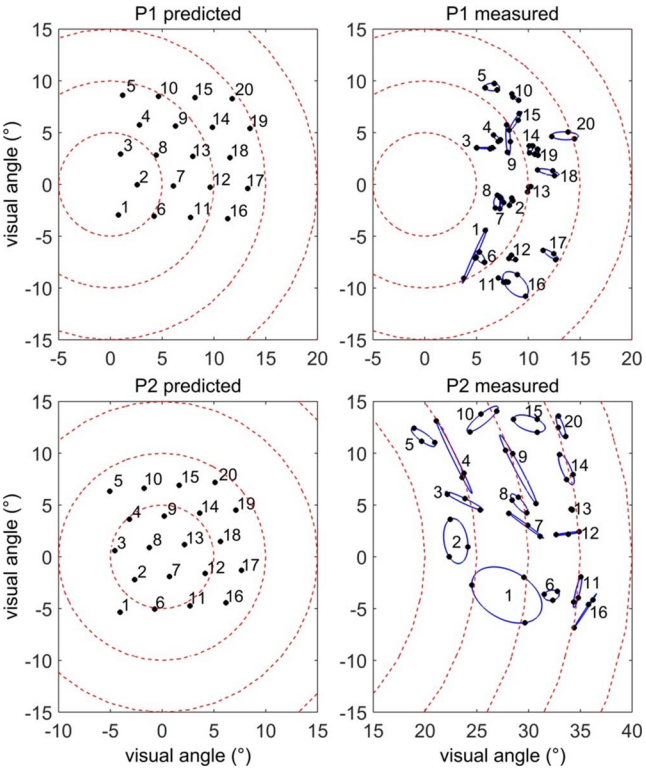

Figure 10. Predicted versus measured phosphene center locations in the visual field for P1 and P2. Predicted locations were calculated from electrode positions on the retina (see Fig. 4) and were inverted vertically to account for the retinotopic mapping to the visual field. Measured locations were recorded using the phosphenes illustrated in Figure 5 (+6 dB) and Figure 6 for P1 and P2, respectively. The three measurements recorded for each electrode were enclosed with a minimum-volume ellipse[39] that covered the three points to indicate the region of the visual field in which the phosphene was reported to occur. The *red circles* are centered on the fovea with radius at 5° intervals.

Phosphene Recognition

The phosphene recognition task was performed with P1 using the +6-dB phosphenes illustrated in Figure 5 and with P2 using the +4-dB phosphenes depicted in Figure 6. Randomized

Table 3. Phosphene Overlap Results for P1

Electrode Spacing, Center-Center	Combinations Tested, *n*	Overlapped	Marginal	Separated
1 mm, adjacent	15	14, 93.3%	1, 6.7%	0, 0%
2 mm	10	3, 30%	7, 70%	0, 0%
3 mm	5	0, 0%	3, 60%	2, 40%

stimulation of each electrode was repeated three times within each run of the task, and three runs were performed with each patient in separate test sessions occurring within 1 month. For P2, electrodes 16, 17, 18, and 19 were excluded from the experiment as either the percept was unreliable (E16) or no percepts could be obtained with those particular stimulation settings. A total of 10 trials for P2 across all recorded blocks (144 trials in total) were rejected from analyses, due to the patient's reporting no phosphene perceived during stimulation (eight trials) or responding with one of the excluded electrodes (two trials), most likely due to lack of attention. No trials were rejected for P1 (180 trials in total).

Figure 11 shows the results grouped according to the spacing offset between the presented electrode and the electrode identified by the patient. An offset of 0 indicates that the patient correctly identified the stimulated electrode, and an offset of 1 indicates that the patient selected an electrode adjacent to that stimulated. Patient 1 correctly identified the stimulated electrode for 57.2% of trials, which far exceeded the chance level of 5% (1/20), and identified an adjacent electrode in 41.1% of trials. Patient 2 correctly identified the stimulated electrode for 23% of trials, which also exceeded the chance level of 6.3% (1/16), and identified an adjacent electrode in 47.1% of trials.

In order to further analyze phosphene recognition as a function of retinotopic location, information transfer scores were calculated to investigate the consistency of the patient's errors. Information transfer analysis[40] is used to measure the extent to which presented information is successfully received by a subject and has been used extensively in speech recognition tasks with auditory prostheses.[41–43] An information transfer score of 0% occurs when the subject's responses are independent of the stimuli presented (i.e., purely random), and a score of 100% is achieved when a given input always results in the same response (i.e., a stimulus is uniquely identifiable). More importantly, information transfer scores have a number of advantages over a percent correct score,[43] including that if stimuli are uniquely identifiable but consistently confused, a high information transfer score will still be obtained. For example, if a subject always responded electrode 1 when electrode 2 was stimulated and vice versa, the percepts are distinctly recognized yet consistently mislabeled. The corresponding percent correct score would be 0%, while the information transfer score would be 100%, indicating that the percepts are uniquely identifiable. The information transfer score for P1 was 70.1%, indicating that the phosphenes were predominantly recognizable and distinguishable. Patient 2's information transfer score was 40.1%, indicating a lower ability to recognize individual phosphenes.

Discussion

The main goal of this study was to characterize the appearance and recognizability of phosphenes elicited using a prototype suprachoroidal retinal prosthesis implanted in three patients with profound vision loss due to RP.

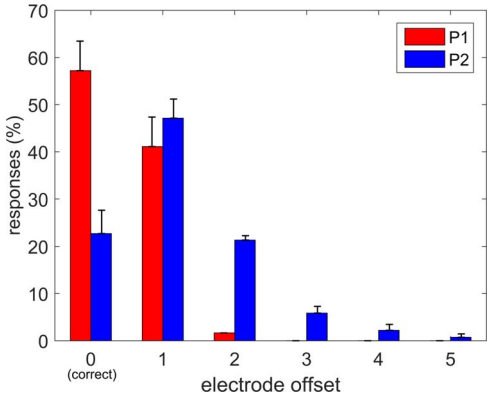

Figure 11. Phosphene recognition results. Patient responses are grouped according to the spacing offset between the stimulated electrode and the electrode identified. *Error bars* correspond to the standard error of the mean for the repeated runs of the task.

Phosphene Complexity and Interpatient Differences

Phosphenes were successfully elicited in all three patients, with the reported appearances varying markedly across patients. A range of factors may be responsible for the interpatient differences observed. While all patients were diagnosed with RP and had light perception vision only (Table 1), differences in the underlying disease subtype and level of disease progression could have caused the degree of neural degeneration and the types (e.g., horizontal, bipolar, amacrine, or ganglion) of surviving retinal neurons to be different for each patient. Furthermore, the constant presence of spontaneous visual percepts and photopsia may also be an indicator that P1, who reported the most detailed and persistent phosphenes, had a more intact visual pathway than the other two patients. Patient 1 reported that, without electrical stimulation, her visual field was always filled with colored swirls that were responsive to light and were of functional use. In contrast, P2 and P3 had only sporadic spontaneous phosphenes, suggesting they may have had less active visual pathways compared to P1. Patients 2 and 3 also both exhibited significant levels of nystagmus, which may have influenced the perception of the phosphenes elicited by electrical stimulation.

The retinotopic location of each electrode may also account for some of the reported complexities in phosphene shape and some interpatient differences. Particularly evident in P1, phosphenes elicited by stimulation of electrodes closer to the fovea had more complex features, in both space and time, compared to those elicited by stimulation of peripheral electrodes. Furthermore, the implant location for P3, who reported all phosphenes as having the same appearance regardless of the electrode stimulated, was farther from the fovea than for P1 and P2 (Fig. 4). These results may likely be attributed to the density and convergence of retinal cell architecture as a function of distance from the fovea, a feature characteristic of most vertebrate retinae.[44] Increased prevalence of one–one correspondence between bipolar–ganglion cell synapses closer to the fovea may have caused a more diverse population of ganglion cells to be activated by a nearby electrode, leading to a more complex retinal output than that elicited from the periphery, where many bipolar cells converge on a single ganglion cell. However, there were still clear differences in the phosphenes reported by each patient for electrodes positioned at comparable distances from the fovea, indicating that the interpatient differences are due to more than just differences in electrode positioning.

Activation of axonal fibers traversing the stimulation sites may also account for some of the complexity of percepts and distortion of phosphene locations, particularly the curved phosphenes perceived by P1. The lower two rows of phosphenes drawn by P1 in Figure 5 all include a component that curves down and to the left. As the optic disc is located to the left of the electrodes corresponding to these percepts (Fig. 4), the shape of the curved components aligns with modeled pathways of retinal axons,[25] suggesting they may be the result of inadvertent axonal activation. However, as the implanted electrodes are located in the suprachoroidal space and the electrical field created by the stimulation permeates the retina as well as the surrounding tissues and fluid, it is uncertain what perceptual effects arose from activation of axons or the residual RGCs and inner neural network.

The complexity in the shape and temporal properties of electrically induced phosphenes and the interpatient variability seen in our study are consistent with reports from other groups who have developed visual prostheses. Phosphenes distinctly differing from a simple round shape have been reported when using other electrode array locations, including epiretinal[18,19] and subretinal[11] placements but also in cortical[8] and optic nerve[13] implants. Phosphenes with multiple spatial components, as seen in P1, have also been reported from other stimulation sites,[8,9,13,15] and phosphenes with light and dark regions, also observed by P1, have been reported with epiretinal stimulation.[20] In another study using a subretinal device, one patient reported seeing arc or movement visual sensations,[11] similar to the moving phosphene descriptions reported by P3. Temporal changes including onset and offset flashes joined by a duller persistent component that can fade out have also been reported with epiretinal stimulation.[21]

Effect of Stimulus Parameters on Phosphenes

We found that stimulation amplitude and rate were the parameters that had the most influence on phosphene appearance. Increasing stimulation amplitude caused phosphenes to appear bigger and brighter, which is consistent with reports from other bionic eye studies.[9,11,18] This was expected, as higher stimulation amplitude would likely excite a larger number of cells spread over a wider area. Increasing the stimulation rate also caused phosphenes to appear brighter and more persistent, especially with P2. However, while higher-rate phosphenes were reported to be fuller, the general shape and size remained similar to those of lower-rate phosphenes. This correlates with observations that have been made using an epiretinal prosthesis,[18] where rate was found to predominantly modulate brightness while amplitude was found to modulate both size and brightness. Increasing the stimulation rate also affected the color of phosphenes reported by P1, with the hue becoming darker bluish or purplish. Stimulation rate has also been shown to influence the color of the percept with epiretinal stimulation (Stanga PE, et al. *IOVS* 2011;52:ARVO E-Abstract 4949; Stanga PE, et al. *IOVS* 2012;53:ARVO E-Abstract 6952). These results suggest that stimulation rate may have affected neuronal selectivity, as different types of RGCs in vitro have been shown to "follow" (i.e., produce at least one spike per pulse) at different maximum stimulus rates,[45–48] with some ON–OFF directionally sensitive RGCs able to follow up to 2000-pps stimuli.[49] Higher rates may have also predominantly stimulated RGCs with less activation of the remaining neural network, or, alternatively, central mechanisms due to integration of multiple stimuli in a short-term window[50] could have led to differences in appearance.

Other stimulation parameters, including phase width, interphase gap, and polarity, did not appear to greatly affect phosphene appearance despite being found to affect threshold levels.[4] The electrode configuration used also did not appear to strongly affect phosphene appearance, despite findings in preclinical studies that configurations with multiple return electrodes (e.g., common ground, hexagonal, pseudo-hexagonal) were able to limit the spread of retinal and cortical activation when compared to monopolar stimulation.[36,51] A caveat to be noted is that in this study and all reported preclinical studies, only single-electrode stimulation was used. Multiple-electrode return configurations may be advantageous when stimulating more than one active electrode, either simultaneously or interleaved in time, as they may reduce interactions. Multiple-electrode stimulation interactions are an area requiring further investigation.

The results obtained suggest that high stimulation rates with a monopolar return are the most effective parameters for producing intense, persistent, and reliable phosphenes with a suprachoroidal retinal prosthesis. The minimal effects of other stimulation pulse parameters suggest that they can be freely adjusted to meet the competing demands of stimulating multiple electrodes interleaved in time, at a high rate within a short time frame, to produce more complex images.

Phosphene Size and Location Within the Visual Field

The drawings produced by P1 and P2 were found to cover large areas of the visual field, suggesting that the phosphenes from suprachoroidal stimulation are larger in comparison to those reported for other implantation sites.[11,13,16,18,19] While this may be true, due to the increased distance between the electrodes and the retinal targets causing greater current spread, it is possible that the sizes of the drawings made by our patients were exaggerated. Studies with other visual prostheses have reported phosphene sizes typically ranging from the size of a pea or matchstick head to the size of a large coin,[2,9,11,15,20] which are more comparable to the anecdotal and caliper-measured sizes reported by our patients.

The results obtained from P1 for the phosphene location and phosphene overlap tasks indicate that her drawings were in fact larger than her perceived phosphenes. For example, the location task results indicate that the phosphene centers for electrodes 3 and 18 were approximately 6° apart. However, in the overlap task, P1 reported these phosphenes to be just touching (marginal overlap). Thus, the phosphenes elicited by electrodes 3 and 18 would have to average approximately 6° wide to be just touching, whereas her corresponding drawings were approximately 10° to 15° wide. Patient 2 also reported that he had considerable difficulty performing the drawing task, and he tended to focus on trying to draw the general shape of the phosphene rather than accurately drawing to scale. The tendency for visually impaired subjects to scale drawings inaccurately has also been observed by Nanduri et al.[19] using a tactile control task. These findings overall suggest that drawing phosphenes may be an inaccurate method for gauging size, but would still be useful in characterizing perceived shapes of phosphenes and other perceived images.

The phosphene locations reported by the patients generally corresponded to the retinotopic electrode positions, albeit with some distortion and displacement. Several factors could have caused the distortion, including the residual state of the visual pathway beneath each electrode and inadvertent axonal activation, as discussed previously. Patient 1 also noted that it was difficult to identify the "center" of complex phosphene shapes, which may have led to some bias. Furthermore, the overlap of several features across phosphenes from nearby electrodes, as seen in her drawings, may have also led to the clustering of locations reported by P1. The discrepancy

between our predicted phosphene locations based on the fundus image and the perceived locations reported by the patients was unexpected, particularly with P2, who indicated a large offset to the right. While P1 did anecdotally report that she perceived her phosphenes slightly to the right of her visual field and her electrode array was located to the right of the fovea, we did not expect the large extent to which the predicted and perceived locations differed. The much larger rightward bias for P2 was even more surprising, as his electrode array was located central to the fovea. Patient 2 anecdotally reported his phosphenes to appear directly in front of him, but consistently identified locations far to the right in the position task. The cause of this discrepancy is unknown and would require further investigation in future patients.

The overlap task results and the observed common features in the drawings from P1 indicate that after the first year of the study, there was considerable overlap between phosphenes from adjacent electrodes (1-mm center–center spacing). While some degree of overlap may be beneficial for combining multiple phosphenes into contiguous images, excessive overlap may mean that some electrodes provide redundant visual percepts. Electrodes spaced farther apart are more likely to produce phosphenes that cover a wider field of view with only marginal overlap, which may make better use of the limited number of electrodes available. The gradual increase in phosphene size over the first year of the study, which correlated with an increase in the electrode-to-retina distance[5] and an increase in perceptual thresholds,[4] would also have increased the degree of overlap. Further work is being undertaken to identify the mechanism behind the increase in electrode-to-retina distance in order to determine ways to prevent the increase in perceptual thresholds and phosphene size. Further work is also required to determine the degree of overlap that would be most beneficial for patients and to determine the optimal electrode spacing for next-generation devices.

The Recognizability of Phosphenes

Despite the complexity and overlapping features of the reported phosphenes, P1 and P2 were remarkably adept at recognizing which electrode was being stimulated. Patients 1 and 2 identified the correct electrode or an adjacent electrode in 98.3% and 70.1% of trials, respectively. These results indicate that a suprachoroidal retinal prosthesis is capable of producing phosphenes with unique features that patients are capable of recognizing. The information available to the patients when trying to identify a given phosphene included its shape, location, temporal properties, and relative intensity, and it is likely that patients used a combination of features to identify electrodes. What is highly encouraging from these results is that all of the features can be of use when patients attempt to functionally use their phosphenes in more complicated psychophysics tasks and for activities of daily living. While an ideal concept for a retinal prosthesis would be an orderly grid of simple punctate phosphenes that can be combined to accurately represent the form of objects, if this cannot be realistically achieved, then phosphenes with recognizably distinct features may have practical utility. For example, phosphenes with distinct features may be used as cues or indicators of the presence or location of obstacles, objects, or people within the visual field, without needing to represent their exact physical form. These features may also be of use when developing image-processing strategies for generating complex and meaningful visual information using phosphenes.

Comparing the overall performance of the patients on all tasks, it is clear that P1 had the most well-defined phosphenes. This may have been due to her phosphenes having greater persistence and more distinct shapes and temporal features than those of the other patients. Patient 2's phosphenes were generally less well-defined blob shapes; and P3, who did not undertake the recognition task, reported that all phosphenes had a similar appearance, regardless of the electrodes stimulated. The extra information available from P1's phosphenes is expected to give her an advantage when undertaking more complicated experimental tasks. In contrast, due to the indistinct nature of his phosphenes, it is expected that P3 would have the most difficulty in undertaking more advanced tasks. This trend has already been observed in a camera-based light localization task,[5] with P1 outperforming P2 and P3.

Feasibility of a Suprachoroidal Retinal Prosthesis

The overall results obtained from this study suggest that the suprachoroidal space is an efficacious site for eliciting phosphenes by electrically stimulating the retina. Phosphenes of varying complexity were successfully obtained from all three visually impaired RP patients tested, demonstrating the efficacy of the implantation site. While the complexity observed in the phosphene appearance will no doubt present numerous challenges when trying to combine multiple phosphenes into meaningful visual information, it may be no greater than the complexity observed from other implantation sites. By characterizing the phosphenes perceived by individual patients, this study also provided valuable insight into factors that may affect patient performance in more advanced psychophysics tasks and when using the implant in a real-time camera-based system. Given that differences in what patients perceive are highly likely to be observed with all implantation sites, proper characterization of an individual's phosphenes when fitting a bionic eye device, along with appropriate training, may be critical in obtaining the best possible outcome for each particular patient.

Acknowledgments

The authors thank the three patients who altruistically volunteered to be implanted with the prototype suprachoroidal retinal implant and generously donated their time for psychophysics testing.

Supported by the Australian Research Council through its Special Research Initiative in Bionic Vision Science and Technology awarded to Bionic Vision Australia and by the Bertalli Family Foundation to the Bionics Institute. The Bionics Institute and the Centre for Eye Research Australia (CERA) acknowledge the support received from the Victorian Government through its Operational Infrastructure Program. CERA is also supported by NHMRC Centre for Clinical Research Excellence Award No. 529923.

Disclosure: **N.C. Sinclair**, None; **M.N. Shivdasani**, None; **T. Perera**, None; **L.N. Gillespie**, None; **H.J. McDermott**, None; **L.N. Ayton**, None; **P.J. Blamey**, None

References

1. Zrenner E, Bartz-Schmidt KU, Benav H, et al. Subretinal electronic chips allow blind patients to read letters and combine them to words. *Proc R Soc Lond B Biol Sci*. 2010; rspb20101747.
2. Fujikado T, Kamei M, Sakaguchi H, et al. Testing of semichronically implanted retinal prosthesis by suprachoroidal-transretinal stimulation in patients with retinitis pigmentosa. *Invest Ophthalmol Vis Sci*. 2011;52:4726–4733.
3. Humayun MS, Dorn JD, da Cruz L, et al. Interim results from the international trial of Second Sight's visual prosthesis. *Ophthalmology*. 2012;119:779–788.

4. Shivdasani MN, Sinclair NC, Dimitrov PN, et al. Factors affecting perceptual thresholds in a suprachoroidal retinal prosthesis. *Invest Ophthalmol Vis Sci*. 2014;55:6467–6481.
5. Ayton LN, Blamey PJ, Guymer RH, et al. First-in-human trial of a novel suprachoroidal retinal prosthesis. *PLoS One*. 2014;9: e115239.
6. Delbeke J, Oozeer M, Veraart C. Position size and luminosity of phosphenes generated by direct optic nerve stimulation. *Vision Res*. 2003;43:1091–1102.
7. Pezaris JS, Reid RC. Demonstration of artificial visual percepts generated through thalamic microstimulation. *Proc Natl Acad Sci U S A*. 2007;104:7670–7675.
8. Brindley GS, Lewin W. The sensations produced by electrical stimulation of the visual cortex. *J Physiol*. 1968;196:479–493.
9. Dobelle W, Mladejovsky M. Phosphenes produced by electrical stimulation of human occipital cortex, and their application to the development of a prosthesis for the blind. *J Physiol*. 1974; 243:553–576.
10. Shepherd RK, Shivdasani MN, Nayagam DA, Williams CE, Blamey PJ. Visual prostheses for the blind. *Trends Biotechnol*. 2013;31:562–571.
11. Wilke R, Gabel V-P, Sachs H, et al. Spatial resolution and perception of patterns mediated by a subretinal 16-electrode array in patients blinded by hereditary retinal dystrophies. *Invest Ophthalmol Vis Sci*. 2011;52:5995–6003.
12. Humayun MS. Pattern electrical stimulation of the human retina. *Vision Res*. 1999;39:2569–2576.
13. Veraart C, Wanet-Defalque MC, Gérard B, Vanlierde A, Delbeke J. Pattern recognition with the optic nerve visual prosthesis. *Artif Organs*. 2003;27:996–1004.
14. Klauke S, Goertz M, Rein S, et al. Stimulation with a wireless intraocular epiretinal implant elicits visual percepts in blind humans. *Invest Ophthalmol Vis Sci*. 2011;52:449–455.
15. Rizzo JF, Wyatt J, Loewenstein J, Kelly S, Shire D. Perceptual efficacy of electrical stimulation of human retina with a microelectrode array during short-term surgical trials. *Invest Ophthalmol Vis Sci*. 2003;44:5362–5369.
16. Chen SC, Suaning GJ, Morley JW, Lovell NH. Simulating prosthetic vision: I. Visual models of phosphenes. *Vision Res*. 2009;49:1493–1506.
17. Thompson RW, Barnett GD, Humayun MS, Dagnelie G. Facial recognition using simulated prosthetic pixelized vision. *Invest Ophthalmol Vis Sci*. 2003;44:5035–5042.
18. Nanduri D, Fine I, Horsager A, et al. Frequency and amplitude modulation have different effects on the percepts elicited by retinal stimulation. *Invest Ophthalmol Vis Sci*. 2012;53:205–214.
19. Nanduri D. *Prosthetic Vision in Blind Human Patients: Predicting the Percepts of Epiretinal Stimulation* [dissertation]. Los Angeles, CA: University of Southern California; 2011.
20. Humayun MS, Weiland JD, Fujii GY, et al. Visual perception in a blind subject with a chronic microelectronic retinal prosthesis. *Vision Res*. 2003;43:2573–2581.
21. Pérez Fornos A, Sommerhalder J, Da Cruz L, et al. Temporal properties of visual perception on electrical stimulation of the retina. *Invest Ophthalmol Vis Sci*. 2012;53:2720–2731.
22. Stensaas SS, Eddington DK, Dobelle WH. The topography and variability of the primary visual cortex in man. *J Neurosurg*. 1974;40:747–755.
23. Drasdo N, Fowler C. Non-linear projection of the retinal image in a wide-angle schematic eye. *Br J Ophthalmol*. 1974;58:709.
24. Fitzgibbon T, Taylor S. Retinotopy of the human retinal nerve fibre layer and optic nerve head. *J Comp Neurol*. 1996;375: 238–251.
25. Fine I, Boynton GM. Pulse trains to percepts: the challenge of creating a perceptually intelligible world with sight recovery technologies. *Phil Trans R Soc B*. 2015;370:20140208.
26. Stronks HC, Dagnelie G. Phosphene mapping techniques for visual prostheses. In: *Visual Prosthetics*. New York: Springer; 2011:367–383.
27. Saunders AL, Williams CE, Heriot W, et al. Development of a surgical procedure for implantation of a prototype suprachoroidal retinal prosthesis. *Clin Experiment Ophthalmol*. 2014; 42:665–674.
28. Villalobos J, Allen PJ, McCombe MF, et al. Development of a surgical approach for a wide-view suprachoroidal retinal prosthesis: evaluation of implantation trauma. *Graefes Arch Clin Exp Ophthalmol*. 2012;250:399–407.
29. Kanda H, Morimoto T, Fujikado T, Tano Y, Fukuda Y, Sawai H. Electrophysiological studies of the feasibility of suprachoroidal-transretinal stimulation for artificial vision in normal and RCS rats. *Invest Ophthalmol Vis Sci*. 2004;45:560–566.
30. Yamauchi Y, Franco LM, Jackson DJ, et al. Comparison of electrically evoked cortical potential thresholds generated with subretinal or suprachoroidal placement of a microelectrode array in the rabbit. *J Neural Eng*. 2005;2:S48.
31. Slater KD, Sinclair NC, Nelson TS, Blamey PJ, McDermott HJ. neuroBi: a highly configurable neurostimulator for a retinal prosthesis and other applications. *IEEE J Transl Eng Health Med*. 2015;3:1–11.
32. Greenwald SH, Horsager A, Humayun MS, Greenberg RJ, McMahon MJ, Fine I. Brightness as a function of current amplitude in human retinal electrical stimulation. *Invest Ophthalmol Vis Sci*. 2009;50:5017–5025.
33. Shannon RV. A model of safe levels for electrical stimulation. *IEEE Trans Biomed Eng*. 1992;39:424–426.
34. Merrill DR, Bikson M, Jefferys JG. Electrical stimulation of excitable tissue: design of efficacious and safe protocols. *J Neurosci Methods*. 2005;141:171–198.
35. Wong Y, Chen S, Seo J, Morley J, Lovell N, Suaning G. Focal activation of the feline retina via a suprachoroidal electrode array. *Vision Res*. 2009;49:825–833.
36. Matteucci PB, Chen SC, Tsai D, et al. Current steering in retinal stimulation via a quasimonopolar stimulation paradigm. *Invest Ophthalmol Vis Sci*. 2013;54:4307–4320.
37. Sabbah N, Authié CN, Sanda N, Mohand-Said S, Sahel J-A, Safran AB. Importance of eye position on spatial localization in blind subjects wearing an Argus II retinal prosthesis. *Invest Ophthalmol Vis Sci*. 2014;55:8259–8266.
38. Dacey DM, Petersen MR. Dendritic field size and morphology of midget and parasol ganglion cells of the human retina. *Proc Natl Acad Sci U S A*. 1992;89:9666–9670.
39. Moshtagh N. Minimum Volume Enclosing Ellipsoid. Matlab Central. Available at: http://au.mathworks.com/matlabcentral/fileexchange/9542-minimum-volume-enclosing-ellipsoid. Accessed June 25, 2015.
40. Miller GA, Nicely PE. An analysis of perceptual confusions among some English consonants. *J Acoust Soc Am*. 1955;27: 338–352.
41. Blamey P, Dowell R, Brown A, Clark GM, Seligman P. Vowel and consonant recognition of cochlear implant patients using formant-estimating speech processors. *J Acoust Soc Am*. 1987; 82:48–57.
42. Blamey PJ, Cowan RS, Alcantara JI, Whitford LA, Clark GM. Speech perception using combinations of auditory visual, and tactile information. *J Rehabil Res Dev*. 1989;26:15–24.
43. Sagi E, Svirsky MA. Information transfer analysis: a first look at estimation bias. *J Acoust Soc Am*. 2008;123:2848–2857.
44. Kolb H. How the retina works. *Am Sci*. 2003;91:28–35.
45. Fried SI, Hsueh H-A, Werblin FS. A method for generating precise temporal patterns of retinal spiking using prosthetic stimulation. *J Neurophysiol*. 2006;95:970–978.
46. Sekirnjak C, Hottowy P, Sher A, Dabrowski W, Litke A, Chichilnisky E. Electrical stimulation of mammalian retinal

Investigative Ophthalmology & Visual Science

ganglion cells with multielectrode arrays. *J Neurophysiol*. 2006;95:3311–3327.

47. Tsai D, Morley JW, Suaning GJ, Lovell NH. Direct activation and temporal response properties of rabbit retinal ganglion cells following subretinal stimulation. *J Neurophysiol*. 2009;102: 2982–2993.
48. Cai C, Ren Q, Desai NJ, Rizzo JF, Fried SI. Response variability to high rates of electric stimulation in retinal ganglion cells. *J Neurophysiol*. 2011;106:153–162.
49. Cai C, Twyford P, Fried S. The response of retinal neurons to high–frequency stimulation. *J Neural Eng*. 2013;10:036009.
50. Watson AB. Temporal sensitivity. In: Boff K, Kaufman L, Thomas J, eds. *Handbook of Perception and Human Performance*. New York, NY: Wiley; 1986:6.1–6.43.
51. Cicione R, Shivdasani MN, Fallon JB, et al. Visual cortex responses to suprachoroidal electrical stimulation of the retina: effects of electrode return configuration. *J Neural Eng*. 2012;9:036009.

Appendix

The Bionic Vision Australia Consortium consists of five member organizations (Centre for Eye Research Australia, Bionics Institute, National Information Communication Technology Australia (NICTA), University of Melbourne, and University of New South Wales) and three partner organizations (The Royal Victorian Eye and Ear Hospital, National Vision Research Institute of Australia, and the University of Western Sydney). For this publication, the consortium members consist of (in alphabetical order) Penelope J. Allen[2], Tamara-Leigh E. Brawn[6], Robert Briggs[2], Anthony N. Burkitt[5], Owen Burns[1], Peter N. Dimitrov[2], Robyn H. Guymer[2], Nigel H. Lovell[4], Chi D. Luu[2], Mark McCombe[2], Michelle E. McPhedran[1], Rodney E. Millard[1], David A.X. Nayagam[1], Nicholas L. Opie[2], Matthew A. Petoe[1], Alexia L. Saunders[1], Peter M. Seligman[1], Kyle D. Slater[1], Robert K. Shepherd[1,3], Gregg J. Suaning[4], Joel Villalobos[1], Chris E. Williams[1,3] and Jonathan Yeoh.[2]

[1]Bionics Institute, East Melbourne, Australia; [2]Centre for Eye Research Australia, The University of Melbourne, Royal Victorian Eye & Ear Hospital, East Melbourne, Australia; [3]Department of Medical Bionics, The University of Melbourne, Carlton, Australia; [4]Department of Biomedical Engineering, University of New South Wales, Kensington, Australia; [5]Department of Electrical and Electronic Engineering, University of Melbourne, Parkville, Australia; and the [6]Bionic Vision Australia, Carlton, Victoria, Australia.

Investigative Ophthalmology & Visual Science